



Published in final edited form as:

Nature. 2020 October ; 586(7830): 567–571. doi:10.1038/s41586-020-2622-0.

SARS-CoV-2 mRNA Vaccine Design Enabled by Prototype Pathogen Preparedness

A full list of authors and affiliations appears at the end of the article.

Summary

A severe acute respiratory syndrome coronavirus (SARS-CoV-2) vaccine is needed to control the global coronavirus infectious disease (COVID-19) public health crisis. Atomic-level structures directed the application of prefusion-stabilizing mutations that improved expression and immunogenicity of betacoronavirus spike proteins¹. Using this established immunogen design, the release of SARS-CoV-2 sequences triggered immediate rapid manufacturing of an mRNA vaccine expressing the prefusion-stabilized SARS-CoV-2 spike trimer (mRNA-1273). Here, we show that mRNA-1273 induces both potent neutralizing antibody responses to wild-type (D614) and D614G mutant² SARS-CoV-2 and CD8 T cell responses and protects against SARS-CoV-2 infection in lungs and noses of mice without evidence of immunopathology. mRNA-1273 is currently in Phase 3 efficacy evaluation.

Since its emergence in December 2019, severe acute respiratory syndrome coronavirus 2 (SARS-CoV-2) has accounted for more than 16 million cases of Coronavirus Disease 2019 (COVID-19) diagnosed worldwide in its first 7 months³. SARS-CoV-2 is the third novel betacoronavirus in the last 20 years to cause substantial human disease; however, unlike its predecessors SARS-CoV and MERS-CoV, SARS-CoV-2 transmits efficiently from person-to-person. In absence of a vaccine, public health measures such as quarantining newly diagnosed cases, contact tracing, and mandating face masks and physical distancing have been instated to reduce transmission⁴. It is estimated that until 60-70% population immunity is established, it is unlikely for COVID-19 to be controlled well enough to resume normal activities. If immunity remains solely dependent on infection, even at a case fatality rate of 1%, >40 million people could succumb to COVID-19 globally⁵. Therefore, rapid

Users may view, print, copy, and download text and data-mine the content in such documents, for the purposes of academic research, subject always to the full Conditions of use:http://www.nature.com/authors/editorial_policies/license.html#terms

* Correspondence and requests for materials should be addressed to Barney S. Graham at bgraham@nih.gov and Andrea Carfi at andrea.carfi@modernatx.com.

Authors have equal contribution to this study

Author Contributions

K.S.C., D.K.E., S.R.L., O.M.A., S.B.B., R.A.G., S.H., A.S., C.Z., A.T.D., K.H.D., S.E., C.A.S., A.W., E.J.F., D.R.M., K.W.B., M.M., B.M.N., G.B.H., K.W., C.H., K.B., D.G.D., L.M., I.R., W.P.K., S.S., L.W., Y.Z., J.C., L.S., L.A.C., E.P., R.J.L., N.E.A., E.N., M.M., V.P., C.L., M.K.L., W.S., K.G., K.L., E.S.Y., A.W., G.A., N.A.D.R., G.S.J., H.B., G.S.A., M.N., T.J.R., M.R.D., I.N.M., K.M.M., J.R.M., R.S.B., A.C., and B.S.G. designed, completed, and/or analyzed experiments. K.S.C., O.M.A., G.B.H., N.W., D.W., J.S.M., and B.S.G. contributed new reagents/analytic tools. K.S.C., K.M.M., and B.S.G. wrote the manuscript. All authors contributed to discussions in regard to and editing of the manuscript.

Competing Interest Declaration

K.S.C., N.W., J.S.M., and B.S.G. are inventors on International Patent Application No. WO/2018/081318 entitled “Prefusion Coronavirus Spike Proteins and Their Use.” K.S.C., O.M.A., G.B.H., N.W., D.W., J.S.M., and B.S.G. are inventors on US Patent Application No. 62/972,886 entitled “2019-nCoV Vaccine”. R.S.B. filed an invention report for the SARS-CoV-2 MA virus (UNC ref. #18752).

development of vaccines against SARS-CoV-2 is critical for changing the global dynamic of this virus.

The spike (S) protein, a class I fusion glycoprotein analogous to influenza hemagglutinin (HA), respiratory syncytial virus (RSV) fusion glycoprotein (F), and human immunodeficiency virus (HIV) gp160 (Env), is the major surface protein on the CoV virion and the primary target for neutralizing antibodies. S proteins undergo dramatic structural rearrangement to fuse virus and host cell membranes, allowing delivery of the viral genome into target cells. We previously showed that prefusion-stabilized protein immunogens that preserve neutralization-sensitive epitopes are an effective vaccine strategy for enveloped viruses, such as RSV⁶⁻¹⁰. Subsequently, we identified 2 proline substitutions (2P) at the apex of the central helix and heptad repeat 1 that effectively stabilized Middle East Respiratory Syndrome (MERS-CoV), SARS-CoV, and human CoV-HKU1 S proteins in the prefusion conformation^{1,11,12}. Similar to other prefusion-stabilized fusion proteins, MERS-CoV S-2P protein was more immunogenic at lower doses than wild-type S protein¹. The 2P has been widely transferrable to other beta-CoV spike proteins, suggesting a generalizable approach for designing stabilized prefusion beta-CoV S vaccine antigens. This is fundamental to the prototype pathogen approach for pandemic preparedness^{13,14}.

Coronaviruses have long been predicted to have a high-likelihood of spill over into humans and cause future pandemics^{15,16}. As part of our pandemic preparedness efforts, we have studied MERS-CoV as prototype pathogen for betacoronaviruses to optimize vaccine design, dissect the humoral immune response to vaccination, and identify mechanisms and correlates of protection. Achieving an effective and rapid vaccine response to a newly emerging virus requires the precision afforded by structure-based antigen design but also a manufacturing platform to shorten time to product availability. Producing cell lines and clinical grade subunit protein typically takes more than 1 year, while manufacturing nucleic acid vaccines can be done in a matter of weeks^{17,18}. In addition to advantages in manufacturing speed, mRNA vaccines are potentially immunogenic and elicit both humoral and cellular immunity¹⁹⁻²¹. Therefore, we evaluated mRNA formulated in lipid nanoparticles (mRNA/LNP) as a delivery vehicle for the MERS-CoV S-2P and found that transmembrane-anchored MERS-CoV S-2P mRNA elicited better pseudovirus neutralizing antibody responses than secreted MERS CoV S-2P (Extended Data Fig. 1a). Additionally, consistent with protein immunogens, MERS CoV S-2P mRNA was more immunogenic than MERS-CoV wild-type S mRNA (Extended Data Fig. 1b). Immunization with MERS CoV S-2P mRNA/LNP elicited potent pseudovirus neutralizing activity down to a 0.1 µg dose and protected hDPP4 transgenic (288/330^{+/+22}) mice against lethal MERS-CoV challenge in a dose-dependent manner, establishing proof-of-concept that mRNA expressing the stabilized S-2P protein is protective. Notably, the sub-protective 0.01 µg dose of MERS-CoV S-2P mRNA did not cause exaggerated disease following MERS-CoV infection, but instead resulted in partial protection against weight loss followed by full recovery without evidence of enhanced illness (Fig. 1).

In early January 2020, a novel CoV (nCoV) was identified as the cause of a respiratory virus outbreak occurring in Wuhan, China. Within 24 hours of the release of the SARS-CoV-2 isolate sequences (then known as “2019-nCoV”) on January 10th, the 2P mutations were

substituted into S positions aa986 and 987 to produce prefusion-stabilized SARS-CoV-2 S (S-2P) protein for structural analysis²³ and serological assay development^{24,25} *in silico* without additional experimental validation. Within 5 days of sequence release, current Good Manufacturing Practice (cGMP) production of mRNA/LNP expressing the SARS-CoV-2 S-2P as a transmembrane-anchored protein with the native furin cleavage site (mRNA-1273) was initiated in parallel with preclinical evaluation. Remarkably, this led to the start of a first in human Phase 1 clinical trial on March 16, 2020, 66 days after the viral sequence was released, and a Phase 2 began 74 days later on May 29, 2020 (Extended Data Fig. 2). Prior to vaccination of the first human subject, expression and antigenicity of the S-2P antigen delivered by mRNA was confirmed *in vitro* (Extended Data Fig. 3), and immunogenicity of mRNA-1273 was documented in several mouse strains. The results of those studies are detailed hereafter.

Immunogenicity was assessed in six-week old female BALB/cJ, C57BL/6J, and B6C3F1/J mice by immunizing intramuscularly (IM) twice with 0.01, 0.1, or 1 μ g of mRNA-1273 at a 3-week interval. mRNA-1273 induced dose-dependent S-specific binding antibodies after prime and boost in all mouse strains (Fig. 2a-c). Potent pseudovirus neutralizing activity was elicited by 1 μ g of mRNA-1273, reaching 819, 89, and 1115 reciprocal IC₅₀ geometric mean titer (GMT) for BALB/cJ, C57BL/6J, and B6C3F1/J mice, respectively (Fig. 2d-f). Pseudovirus neutralizing activity in 1 μ g mRNA-1273-immunized mice was similar comparing homotypic Wuhan-1 pseudovirus expressing spike with the S D614G substitution, which has recently become dominant around the world² (Extended Data Fig. 4). To further gauge immunogenicity across a wide dose range, BALB/c mice were immunized with 0.0025 – 20 μ g of mRNA-1273 revealing a strong positive correlation between dose-dependent mRNA-1273-elicited binding and pseudovirus neutralizing antibody responses (Extended Data Fig. 5). BALB/cJ mice that received a single dose of mRNA-1273 were evaluated in order to ascertain the utility for a one-dose vaccine regimen. S-binding antibodies were induced in mice immunized with one dose of 1 or 10 μ g of mRNA-1273, and the 10 μ g dose elicited pseudovirus neutralizing antibody activity that increased between week 2 and week 4, reaching 315 reciprocal IC₅₀ GMT (Extended Data Fig. 6a-b). These data demonstrate that mRNA expressing SARS-CoV-2 S-2P is a potent immunogen and pseudovirus neutralizing activity can be elicited with a single dose.

Next, we evaluated the balance of Th1 and Th2, because vaccine-associated enhanced respiratory disease (VAERD) has been associated with Th2-biased immune responses in children immunized with whole-inactivated virus vaccines against RSV and measles virus^{26,27}. A similar phenomenon has also been reported in some animal models with whole-inactivated and other types of experimental SARS-CoV vaccines²⁸⁻³⁰. Thus, we first compared levels of S-specific IgG2a/c and IgG1, which are surrogates of Th1 and Th2 responses respectively, elicited by mRNA-1273 to those elicited by SARS-CoV-2 S-2P protein adjuvanted with the TLR4-agonist Sigma Adjuvant System (SAS). Both immunogens elicited IgG2a and IgG1 subclass S-binding antibodies, indicating a balanced Th1/Th2 response (Fig. 3a-c; Extended Data Fig. 7). The S-specific IgG subclass profile following a single dose of mRNA-1273 (Extended Data Fig. 6c) was similar to that observed following two doses. In contrast, Th2-biased antibodies with lower IgG2a/IgG1 subclass response ratios were observed in mice immunized with SARS-CoV-2 S-2P protein

formulated in alum (Extended Data Fig. 8a-b). Following re-stimulation with peptide pools (S1 and S2) corresponding to the S protein, splenocytes from mRNA-1273-immunized mice secreted more IFN- γ than IL-4, IL-5, or IL-13 whereas SARS-CoV-2 S-2P protein with alum induced Th2-skewed cytokine secretion (Extended Data Fig. 8c-d). 7 weeks post-boost, we also directly measured cytokine patterns in vaccine-induced memory T cells by intracellular cytokine staining (ICS); mRNA-1273-elicited CD4+ T cells re-stimulated with S1 or S2 peptide pools exhibited a Th1-dominant response, particularly at higher immunogen doses (Fig. 3d-e). Furthermore, 1 μ g of mRNA-1273 induced a robust CD8+ T cell response to the S1 peptide pool (Fig. 3f-g). The Ig subclass and T cell cytokine data together demonstrate that immunization with mRNA-1273 elicits a balanced Th1/Th2 response in contrast to the Th2-biased response seen with S protein adjuvanted with alum, suggesting that mRNA vaccination avoids Th2-biased immune responses that have been linked to VAERD.

Protective immunity was assessed in young adult BALB/cJ mice challenged with mouse-adapted (MA) SARS-CoV-2. SARS-CoV-2 MA contains RBD substitutions Q498Y/P499T generated via site-directed mutagenesis in an infectious clone³¹. The substitutions effectively allow binding of the virus to the mouse ACE2 receptor and infection and replication in the upper and lower respiratory tract³². BALB/cJ mice that received two 1 μ g doses of mRNA-1273 were completely protected from viral replication in lungs after challenge at a 5- (Fig. 4a) or 13-week intervals following boost (Extended Data Fig. 9a). mRNA-1273-induced immunity also rendered viral replication in nasal turbinates undetectable in 6 out of 7 mice (Fig. 4b, Extended Data Fig. 9b). Efficacy of mRNA-1273 was dose-dependent, with two 0.1 μ g mRNA-1273 doses reducing lung viral load by ~100-fold and two 0.01 μ g mRNA-1273 doses reducing lung viral load by ~3-fold (Fig. 4a). Of note, mice challenged 7 weeks after a single dose of 1 or 10 μ g of mRNA-1273 were also completely protected against lung viral replication (Fig. 4c). Challenging animals immunized with sub-protective doses provides an orthogonal assessment of safety signals, such as increased clinical illness or pathology. Similar to what was observed with MERS-CoV S-2P mRNA, mice immunized with sub-protective 0.1 and 0.01 μ g mRNA-1273 doses showed no evidence of enhanced lung pathology or excessive mucus production (Fig. 4d). In summary, mRNA-1273 is immunogenic, efficacious, and does not show evidence of promoting VAERD when given at sub-protective doses in mice.

Here, we showed that 1 μ g of mRNA-1273 was sufficient to induce robust pseudovirus neutralizing activity and CD8 T cell responses, balanced Th1/Th2 antibody isotype responses, and protection from viral replication for more than 3 months following a prime/boost regimen similar to that being tested in humans. The level of pseudovirus neutralizing activity induced by 1 μ g of mRNA-1273 in mice is similar in magnitude to that induced in human subjects by 100 μ g³³, which is the dose level chosen for mRNA-1273 to advance into phase 3 clinical trials. Inclusion of lower sub-protective doses demonstrated the dose-dependence of antibody, Th1 CD4 T cell responses, and protection, suggesting immune correlates of protection can be further elucidated. A major goal of animal studies to support SARS-CoV-2 vaccine candidates through clinical trials is to not only prove elicitation of potent protective immune responses, but to show that sub-protective responses do not cause VAERD⁵. Sub-protective doses did not prime mice for enhanced immunopathology

following challenge. Moreover, the induction of protective immunity following a single dose suggests that consideration could be given to administering one dose of this vaccine in the outbreak setting. These data, combined with immunogenicity data from nonhuman primates and subjects in early Phase 1 clinical trials, were used to inform the dose and regimen of mRNA1273 in advanced clinical efficacy trials.

The COVID-19 pandemic of 2020 is the Pathogen X event that has long been predicted^{13,14}. Here, we provide a paradigm for rapid vaccine development. Structure-guided stabilization of the MERS-CoV S protein combined with a fast, scalable, and safe mRNA/LNP vaccine platform led to a generalizable beta-CoV vaccine solution that translated into a commercial mRNA vaccine delivery platform, paving the way for the rapid response to the COVID-19 outbreak. This is a demonstration of how the power of new technology-driven concepts like synthetic vaccinology facilitate a vaccine development program that can be initiated with pathogen sequences alone¹¹. It is also a proof-of-concept for the prototype pathogen approach for pandemic preparedness and response that is predicated on identifying generalizable solutions for medical countermeasures within virus families or genera¹³. Even though the response to the COVID-19 pandemic is unprecedented in its speed and breadth, we envision a response that could be quicker. There are 24 other virus families known to infect humans, and with sustained investigation of those potential threats, we could be better prepared for future looming pandemics¹⁴.

Methods

Pre-clinical mRNA-1273 mRNA and LNP Production Process

A sequence-optimized mRNA encoding prefusion-stabilized SARS-CoV-2 S-2P protein was synthesized *in vitro* using an optimized T7 RNA polymerase-mediated transcription reaction with complete replacement of uridine by N1m-pseudouridine³⁴. The reaction included a DNA template containing the immunogen open-reading frame flanked by 5' UTR and 3' UTR sequences and was terminated by an encoded polyA tail. After transcription, the Cap 1 structure was added to the 5' end using Vaccinia capping enzyme (New England Biolabs) and Vaccinia 2'O-methyltransferase (New England Biolabs). The mRNA was purified by oligo-dT affinity purification, buffer exchanged by tangential flow filtration into sodium acetate, pH 5.0, sterile filtered, and kept frozen at -20 °C until further use.

The mRNA was encapsulated in a lipid nanoparticle through a modified ethanol-drop nanoprecipitation process described previously²⁰. Briefly, ionizable, structural, helper, and PEG lipids were mixed with mRNA in acetate buffer, pH 5.0, at a ratio of 2.5:1 (lipids:mRNA). The mixture was neutralized with Tris-Cl, pH 7.5, sucrose was added as a cryoprotectant, and the final solution was sterile filtered. Vials were filled with formulated LNP and stored frozen at -70 °C until further use. The drug product underwent analytical characterization, which included the determination of particle size and polydispersity, encapsulation, mRNA purity, double stranded RNA content, osmolality, pH, endotoxin, and bioburden, and the material was deemed acceptable for *in vivo* study.

MERS-CoV and SARS-CoV Protein Expression and Purification

Vectors encoding MERS-CoV S-2P¹ and SARS-CoV S-2P²³ were generated as previously described with the following small amendments. Proteins were expressed by transfection of plasmids into Expi293 cells using Expifectamine transfection reagent (ThermoFisher) in suspension at 37°C for 4-5 days. Transfected cell culture supernatants were collected, buffer exchanged into 1X phosphate buffered saline (PBS), and protein was purified using Strep-Tactin resin (IBA). For proteins used for mouse inoculations, tags were cleaved with addition of HRV3C protease (ThermoFisher) (1% wt/wt) overnight at 4 °C. Size exclusion chromatography using Superose 6 Increase column (GE Healthcare) yielded final purified protein.

Design and Production of Recombinant Minifibrin Foldon Protein

A mammalian codon-optimized plasmid encoding foldon inserted minifibrin (ADIVLNDLPFVDGPPAEGQSRISWIKNGEEILGADTQYGSEGSMMNRPTVSVLRNVEVLDKNIGILKTSLETANSDIKTIQEAGYIPEAPRDGQAYVRKDGWVLLSTFLSPALVPRGSHHHHHHSAWHPQFEK) with a C-terminal thrombin cleavage site, 6x His-tag, and Strep-TagII was synthesized and subcloned into a mammalian expression vector derived from pLEXm. The construct was expressed by transient transfection of Expi293 (ThermoFisher) cells in suspension at 37°C for 5 days. The protein was first purified with a Ni²⁺-nitrilotriacetic acid (NTA) resin (GE Healthcare,) using an elution buffer consisting of 50 mM Tris-HCl, pH 7.5, 400 mM NaCl, and 300 mM imidazole, pH 8.0, followed by purification with StrepTactin resin (IBA) according to the manufacturer's instructions.

Cell Lines

HEK293T/17 (ATCC #CRL-11268), Vero E6 (ATCC), Huh7.5 cells (provided by Deborah R. Taylor, US Food and Drug Administration), and ACE2-expressing 293T cells (provided by Michael Farzan, Scripps Research Institute) were cultured in Dulbecco's modified Eagle's medium (DMEM) supplemented with 10% FBS, 2 mM glutamine, and 1% penicillin/streptomycin at 37°C and 5% CO₂. Vero E6 cells used in plaque assays to determine lung and nasal turbinate viral titers were cultured in DMEM supplemented with 10% Fetal Clone II and 1% anti/anti at 37°C and 5% CO₂. Vero E6 cells used in PRNT assays were cultured in DMEM supplemented with 10% Fetal Clone II and amphotericin B [0.25 µg/ml] at 37C and 5% CO₂. Lentivirus encoding hACE2-P2A-TMPRSS2 was made to generate A549-hACE2-TMPRSS2 cells which were maintained in DMEM supplemented with 10% FBS and 1 µg/mL puromycin. Expi293 cells were maintained in manufacturer's suggested media. Cell lines were not authenticated. All cells lines were tested for mycoplasma.

In vitro mRNA Expression

HEK293T cells were transiently transfected with mRNA encoding SARS-CoV-2 WT S or S-2P protein using a TranIT mRNA transfection kit (Mirus). After 24 hr, the cells were harvested and resuspended in FACS buffer (1X PBS, 3% FBS, 0.05% sodium azide). To detect surface protein expression, the cells were stained with 10 µg/mL ACE2-FLAG (Sigma) or 10 µg/mL CR3022³⁵ in FACS buffer for 30 min on ice. Thereafter, cells were

washed twice in FACS buffer and incubated with FITC anti-FLAG (Sigma) or Alexafluor 647 goat anti-human IgG (Southern Biotech) in FACS buffer for 30 min on ice. Live/Dead aqua fixable stain (Invitrogen) were utilized to assess viability. Data acquisition was performed on a BD LSRII Fortessa instrument (BD Biosciences) and analyzed by FlowJo software v10 (Tree Star, Inc.)

Mouse Models

Animal experiments were carried out in compliance with all pertinent US National Institutes of Health regulations and approval from the Animal Care and Use Committee of the Vaccine Research Center, Moderna Inc., or University of North Carolina at Chapel Hill. For immunogenicity studies, 6-8-week-old female BALB/c (Charles River), BALB/cJ, C57BL/6J, or B6C3F1/J mice (Jackson Laboratory) were used. mRNA formulations were diluted in 50 μ L of 1X PBS, and mice were inoculated IM into the same hind leg for both prime and boost. Control mice received PBS because prior studies have demonstrated the mRNA formulations being tested do not create significant levels of non-specific immunity beyond a few days³⁶⁻³⁸. For all SARS-CoV-2 S-P protein vaccinations, mice were inoculated IM, with SAS, as previously detailed¹. For S-2P + alum immunizations, SARS-CoV-2 S-2P protein + 250 μ g alum hydrogel was delivered IM. For challenge studies to evaluate MERS-CoV-2 vaccines, 16-20-week-old male and female 288/330^{+/+}mice²² were immunized. Four weeks post-boost, pre-challenge sera were collected from a subset of mice, and remaining mice were challenged with 5×10^5 PFU of a mouse-adapted MERS-CoV EMC derivative, m35c4³⁹. On day 3 post-challenge, lungs were harvested, and hemorrhage and viral titer were assessed, per previously published methods⁴⁰. For challenge studies to evaluate SARS-CoV-2 vaccines, BALB/cJ mice were challenged with 10^5 PFU of mouse-adapted SARS-CoV-2 (SARS-CoV-2 MA). This virus contains two mutations (Q498T/P499Y) in the receptor binding domain (RBD) that allow binding of SARS-CoV-2 spike to the mouse angiotensin-converting enzyme 2 (ACE2) receptor and infection and replication in the upper and lower respiratory tract³². On day 2 post-challenge, lungs and nasal turbinates were harvested for viral titer assessment, per previously published methods³². Sample size for animal experiments was determined based on criteria set by institutional ACUC. Experiments were not randomized or blinded.

Histology

Lungs from mice were collected at the indicated study endpoints and placed in 10% neutral buffered formalin (NBF) until adequately fixed. Thereafter, tissues were trimmed to a thickness of 3-5 mm, processed and paraffin embedded. The respective paraffin tissue blocks were sectioned at 5 μ m and stained with hematoxylin and eosin (H&E). All sections were examined by a board-certified veterinary pathologist using an Olympus BX51 light microscope and photomicrographs were taken using an Olympus DP73 camera.

Enzyme-linked Immunosorbent Assay (ELISA)

Nunc Maxisorp ELISA plates (ThermoFisher) were coated with 100 ng/well of protein in 1X PBS at 4°C for 16 hr. Where applicable, to eliminate fold-on-specific binding from MERS-CoV S-2P- or SARS-CoV-2 S-2P protein-immune mouse serum, 50 μ g/mL of fold-on protein was added for 1 hr at room temperature (RT). After standard washes and blocks,

plates were incubated with serial dilutions of heat-inactivated (HI) sera for 1 hr at RT. Following washes, anti-mouse IgG, IgG1, or IgG2a and/or IgG2c-horseradish peroxidase conjugates (ThermoFisher) were used as secondary Abs, and 3,3',5'-tetramethylbenzidine (TMB) (KPL) was used as the substrate to detect Ab responses. Endpoint titers were calculated as the dilution that emitted an optical density exceeding 4X background (secondary antibody alone).

Lentivirus-based Pseudovirus Neutralization Assay

The pseudovirus neutralization assay measures the inhibition of pseudovirus attachment and entry including fusion-inhibiting activity. It is a single-round virus, does not replicate, and does not express the S protein in transduced cells. Therefore, pseudovirus infection will not cause cell-to-cell fusion or plaque formation that can be measured in a classical neutralization assay using live virus. This pseudovirus neutralization assay has been shown to correlate with live virus plaque reduction neutralization³³, and because it does not require BL3 containment, was chosen as the preferred assay for measuring neutralizing activity in these studies. We introduced divergent amino acids, as predicted from translated sequences, into the CMV/R-MERS-CoV EMC S (GenBank#: [AFS88936](#)) gene⁴¹ to generate a MERS-CoV m35c4 S gene³⁹. To produce SARS-CoV-2 pseudoviruses, a codon-optimized CMV/R-SARS-CoV-2 S (Wuhan-1, Genbank #: [MN908947.3](#)) plasmid was constructed. Pseudoviruses were produced by co-transfection of plasmids encoding a luciferase reporter, lentivirus backbone, and S genes into HEK293T/17 cells (ATCC #CRL-11268), as previously described⁴¹. For SARS-CoV-2 pseudovirus, human transmembrane protease serine 2 (TMPRSS2) plasmid was also co-transfected⁴². Pseudoneutralization assay methods have been previously described^{1,33}. Briefly, heat-inactivated (HI) serum was mixed with pseudoviruses, incubated, and then added to Huh7.5 cells or ACE-2-expressing 293T cells, for MERS-CoV and SARS-CoV-2 respectively. Seventy-two hr later, cells were lysed, and luciferase activity (relative light units, RLU) was measured. Percent neutralization was normalized considering uninfected cells as 100% neutralization and cells infected with only pseudovirus as 0% neutralization. IC₅₀ titers were determined using a log (agonist) vs. normalized response (variable slope) nonlinear function in Prism v8 (GraphPad).

Recombinant VSV G-based Pseudovirus Neutralization Assay

Codon-optimized wild-type (D614) or D614G spike gene (Wuhan-Hu-1 strain, NCBI Reference Sequence #: NC_045512.2) was cloned into pCAGGS vector. To generate VSV G-based SARS-CoV-2 pseudovirus, BHK-21/WI-2 cells were transfected with the spike expression plasmid and infected VSV G-firefly-luciferase as previously described⁴³. A549-hACE2-TMPRSS2 cells were infected by pseudovirus for 1 hr at 4°C. The inoculum virus or virus-antibody mix was removed after infection. 18 hr later, equal volume of One-Glo reagent (Promega) was added to culture medium for readout using BMG PHERastar-FS plate reader. The neutralization procedure and data analysis are same as mentioned above in the lentivirus-based pseudovirus neutralization assay.

Plaque Reduction Neutralization Test (PRNT)

HI sera were diluted in gelatin saline (0.3% [wt/vol] gelatin in phosphate-buffered saline supplemented with CaCl₂ and MgCl₂) to generate a 1:5 dilution of the original specimen,

which served as a starting concentration for further serial log₄ dilutions terminating in 1:81,920. Sera were combined with an equal volume of SARS-CoV-2 clinical isolate 2019-nCoV/USA-WA1-F6/2020 in gelatin saline, resulting in an average concentration of 730 plaque-forming units per mL (determined from plaque counts of 24 individual wells of untreated virus) in each serum dilution. Thus, final serum concentrations ranged from 1:10 to 1:163,840 of the original. Virus/serum mixtures were incubated for 20 min at 37 °C, followed by adsorption of 0.1 mL to each of two confluent Vero E6 cell monolayers (in 10-cm² wells) for 30 min at 37°C. Cell monolayers were overlaid with Dulbecco's modified Eagle's medium (DMEM) containing 1% agar and incubated for 3 d at 37°C in humidified 5% CO₂. Plaques were enumerated by direct visualization. The average number of plaques in virus/serum (duplicate) and virus-only (24) wells was used to generate percent neutralization curves according to the following formula: 1 – (ratio of mean number of plaques in the presence and absence of serum). The PRNT IC₅₀ titer was defined as the reciprocal serum dilution at which the neutralization curve crossed the 50% threshold.

Intracellular Cytokine Staining

Mononuclear single cell suspensions from whole mouse spleens were generated using a gentleMACS tissue dissociator (Miltenyi Biotec) followed by 70 µm filtration and density gradient centrifugation using Fico/Lite-LM medium (Atlanta Biologicals). Cells from each mouse were resuspended in R10 media (RPMI 1640 supplemented with Pen-Strep antibiotic, 10% HI-FBS, Glutamax, and HEPES) and incubated for 6 hr at 37°C with protein transport inhibitor cocktail (eBioscience) under three conditions: no peptide stimulation, and stimulation with two spike peptide pools (JPT product PM-WCPV-S-1). Peptide pools were used at a final concentration of 2 µg/mL each peptide. Cells from each group were pooled for stimulation with cell stimulation cocktail (eBioscience) as a positive control. Following stimulation, cells were washed with PBS prior to staining with LIVE/DEAD Fixable Blue Dead Cell Stain (Invitrogen, cat. L23105, 1/800) for 20 min at RT. Cells were then washed in FC buffer (PBS supplemented with 2% HI-FBS and 0.05% NaN₃) and resuspended in BD Fc Block (BD, cat. 553141, clone 2.4G2, 1/100) for 5 min at RT prior to staining with a surface stain cocktail containing the following antibodies: I-A/I-E PE (BD, cat. 557000, clone M5/114.15.2, 1/2500), CD8a BUV805 (BD, cat. 612898, clone 53-6.7, 1/80), CD44 BUV395 (BD, cat. 740215, clone IM7, 1/800), CD62L BV605 (Biolegend, cat. 104418, clone MEL-14, 1/5000), and CD4 BV480 (BD, cat. 565634, clone RM4-5, 1/500) in brilliant stain buffer (BD). After 15 min, cells were washed with FC buffer then fixed and permeabilized using the BD Cytotfix/Cytoperm fixation/permeabilization solution kit according to manufacturer instructions. Cells were washed in perm/wash solution and stained with Fc Block (5 min at RT), followed by intracellular staining (30 min at 4°C) using a cocktail of the following antibodies: CD3e BUV737 (BD, cat. 741788, clone 17A2, 1/80), IFN-γ BV650 (BD, cat. 563854, clone XMG1.2, 1/500), TNF-α BV711 (BD, cat. 563944, clone MP6-XT22, 1/80), IL-2 BV421 (BD, cat. 562969, clone JES6-5H4, 1/80), IL-4 Alexa Fluor 488 (Biolegend, cat. 504109, clone 11B11, 1/80), and IL-5 APC (Biolegend, cat. 504306, clone TRFK5, 1/320) in 1x perm/wash diluted with brilliant stain buffer. Finally, cells were washed in perm/wash solution and resuspended in 0.5% PFA-FC stain buffer prior to running on a Symphony A5 flow cytometer (BD). Analysis was performed using FlowJo software, version 10.6.2 according to the gating strategy outlined in Extended Data Fig. 10.

Background cytokine expression in the no peptide condition was subtracted from that measured in the S1 and S2 peptide pools for each individual mouse.

T Cell Stimulation and Cytokine Analysis

Spleens from immunized mice were collected 2 weeks post-boost. 2×10^6 splenocytes/well (96-well plate) were stimulated *in vitro* with two peptide libraries, JPT1 and JPT2, (15mers with 11 aa overlap) covering the entire SARS-CoV-2 spike protein (JPT product PM-WCPV-S-1). Both peptide libraries were used at a final concentration of $1 \mu\text{g/mL}$. After 24 hr of culture at 37°C , the plates were centrifuged and supernatant was collected and frozen at -80°C for cytokine detection. Measurements and analyses of secreted cytokines from a murine 35-plex kit were performed using a multiplex bead-based technology (Luminex) assay with a Bio-Plex 200 instrument (Bio-Rad) after 2-fold dilution of supernatants.

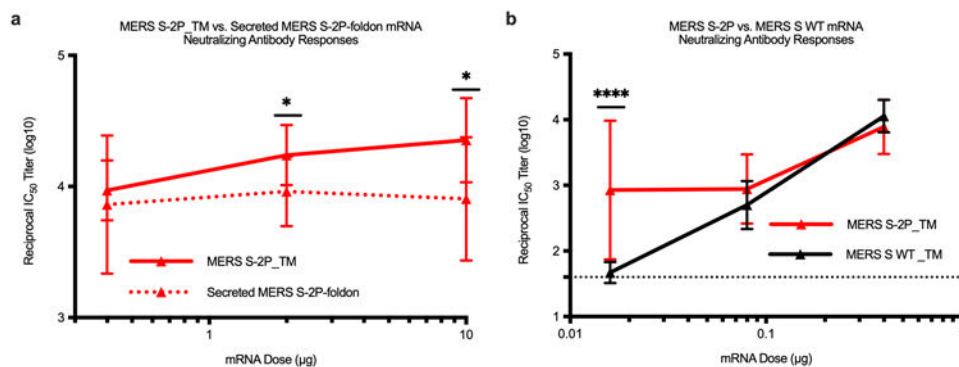
Statistical Analysis

Geometric means or arithmetic means are represented by the heights of bars, or symbols, and error bars represent the corresponding SD. Dotted lines indicate assay limits of detection. Two-sided Mann-Whitney tests were used to compare 2 experimental groups and two-sided Wilcoxon signed-rank tests to compare the same animals at different time points. To compare >2 experimental groups, Kruskal-Wallis ANOVA with Dunn's multiple comparisons tests were applied. In Extended Data Fig. 5a-b, all doses were compared to the $20 \mu\text{g}$ dose by two-sided Mann-Whitney test in a stepwise fashion, such that lowest doses were tested first at $\alpha = 0.05$ and higher doses tested only if the lower doses were significant. In Extended Data Fig. 5c, a Spearman correlation test was used to correlate binding antibody titers to pseudovirus neutralizing antibody titers. Statistical analyses were performed using R v4.0.0 or Prism v8 (GraphPad). * = p-value < 0.05 , ** = p-value < 0.01 , *** = p-value < 0.001 , **** = p-value < 0.0001 .

Data Availability Statement

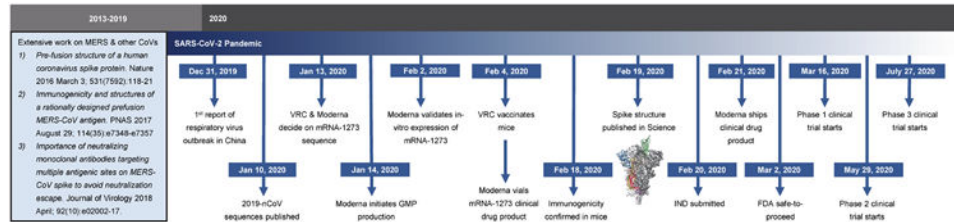
The authors declare that the data supporting the findings of this study are available within the paper and its supplementary information files.

Extended Data



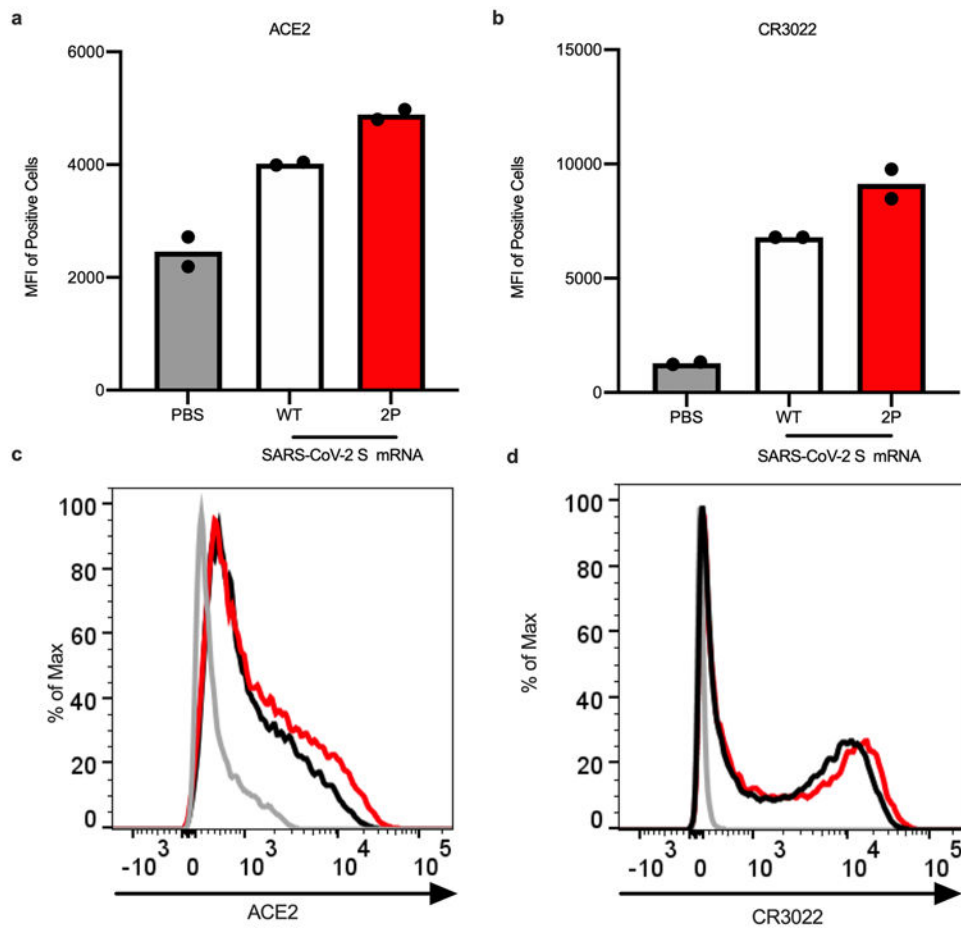
Extended Data Figure 1. Transmembrane-anchored MERS-CoV S-2P (S-2P_TM) mRNA elicits more potent pseudovirus neutralizing antibody responses than secreted MERS-CoV S-2P and S WT mRNA.

C57BL/6J mice (n=10/group) were immunized at weeks 0 and 4 with (a) 0.4, 2, or 10 μg of MERS-CoV S-2P_TM (red) or MERS S-2P_secreted (red hashed) or (b) 0.016 μg , 0.08 μg , or 0.4 μg of MERS-CoV S-2P or MERS-CoV S WT_TM (black) mRNA. Sera were collected 4 weeks post-boost and assessed for neutralizing antibodies against MERS-CoV m35c4 pseudovirus. Immunogens were compared at each dose level by two-sided Mann-Whitney test. * = p-value < 0.05, **** = p-value < 0.0001. Data are presented as GMT +/- geometric SD.

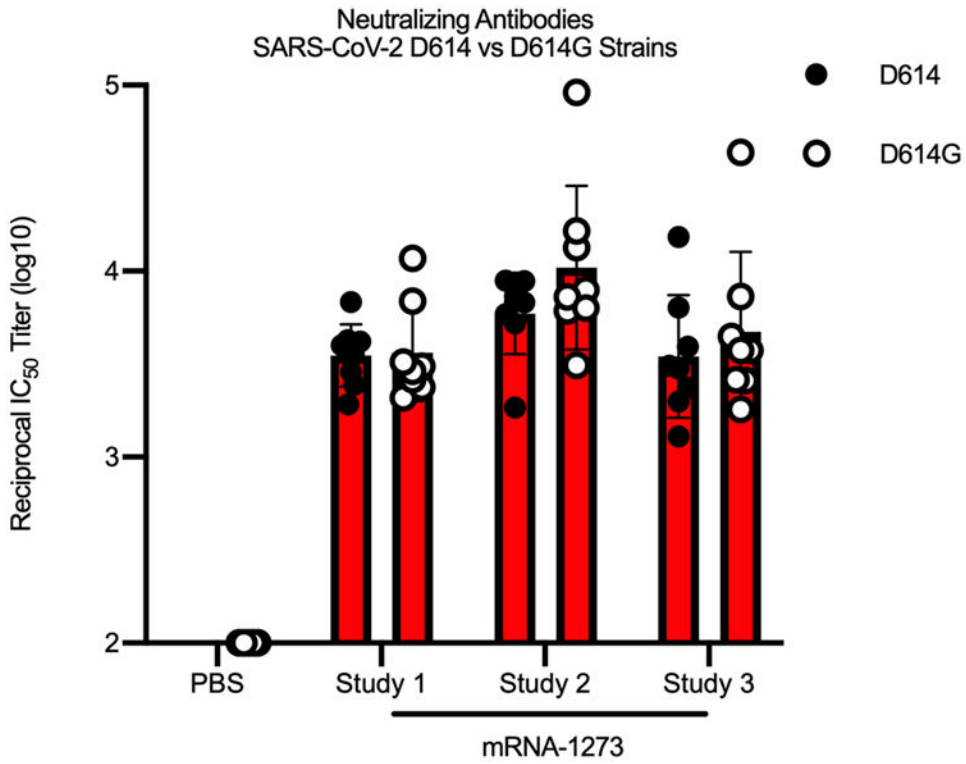


Extended Data Figure 2. Timeline for mRNA-1273's progression to clinical trial.

The morning after novel coronavirus (nCoV) sequences were released, spike sequences were modified to include prefusion stabilizing mutations and synthesized for protein production, assay development, and vaccine development. Twenty-five days after viral sequences were released, clinically-relevant mRNA-1273 was received to initiate animal experiments. Immunogenicity in mice was confirmed 15 days later. Moderna shipped clinical drug product 41 days after GMP production began, leading to the Phase 1 clinical trial starting 66 days following the release of nCoV sequences.

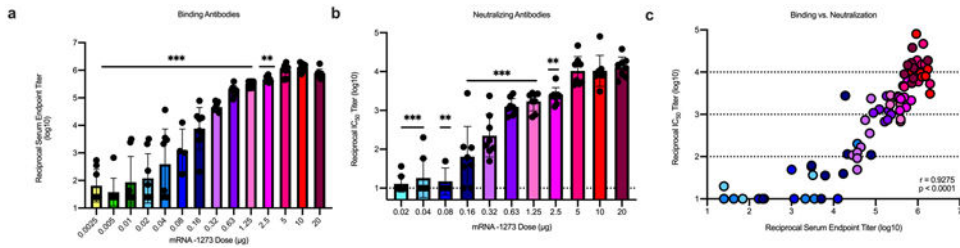


Extended Data Figure 3. *In vitro* expression of SARS-CoV-2 spike mRNA on cell surface. 293T cells were transfected in duplicate with mRNA expressing SARS-CoV-2 wild-type spike (white bars, black lines) or S-2P (red), stained with ACE2 (a,c) or CR3022 (b,d), and evaluated by flow cytometry 24 post-transfection. Mock-transfected (PBS) cells served as a control (gray). (a-b) Data are presented as mean.



Extended Data Figure 4. mRNA-1273 elicits robust pseudovirus neutralizing antibody responses to SARS-CoV-2_D614G.

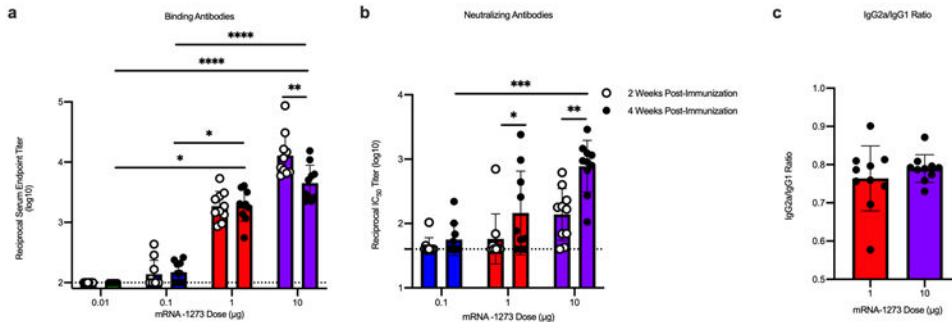
BALB/c mice (n=8/group) were immunized at weeks 0 and 3 weeks with 1 µg (red) of mRNA-1273, in three individual studies, or PBS (n=5). Sera were collected 2 weeks post-boost and assessed for neutralizing antibodies against homotypic SARS-CoV-2_D614 pseudovirus (filled circles) or SARS-CoV-2_D614G (unfilled circles). Comparisons between D614 and D614G were made by two-sided Mann-Whitney test within each study, and no significance was detected. Data are presented as GMT +/- geometric SD.



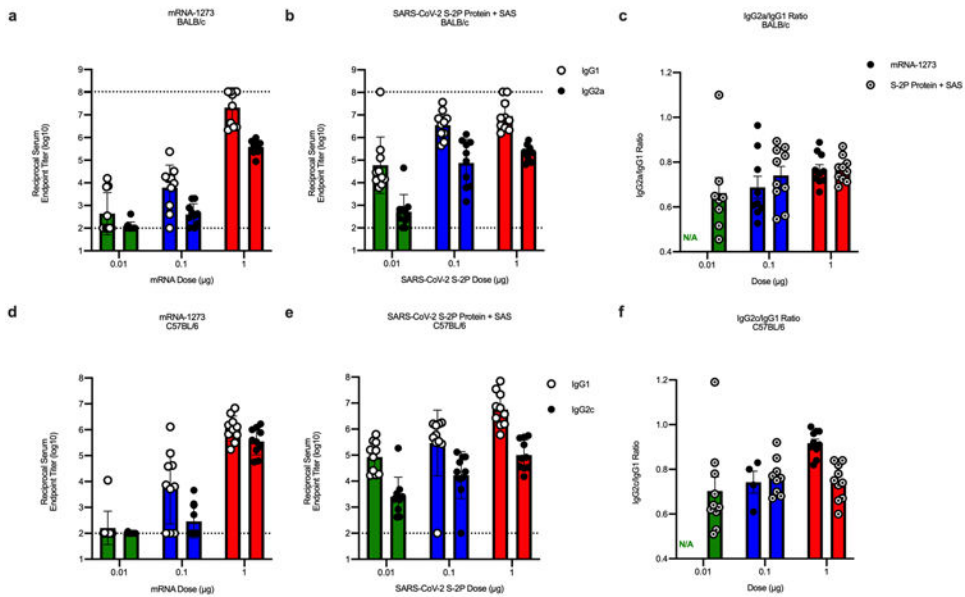
Extended Data Figure 5. Dose-dependent mRNA-1273-elicited antibody responses reveal strong positive correlation between binding and pseudovirus neutralization titers.

BALB/cJ mice (n=10/group) were immunized at weeks 0 and 3 weeks with various doses (0.0025 – 20 µg) of mRNA-1273. Sera were collected 2 weeks post-boost and assessed for SARS-CoV-2 S-specific IgG by ELISA (a) and neutralizing antibodies against homotypic SARS-CoV-2 pseudovirus (b). (a-b) All doses were compared to the 20 µg dose by two-sided Mann-Whitney test in a stepwise fashion, such that lowest doses were tested first at $\alpha = 0.05$ and higher doses tested only if the lower doses were significant. Data are presented as

GMT +/- geometric SD, and dotted lines represent assay limits of detection. (c) Spearman correlation test was used to correlate binding antibody titers to pseudovirus neutralizing antibody titers (p < 0.0001). Each dot represents an individual mouse. Dotted lines highlight log₁₀ IC₅₀ boundaries. ** = p-value < 0.01, *** = p-value < 0.001.

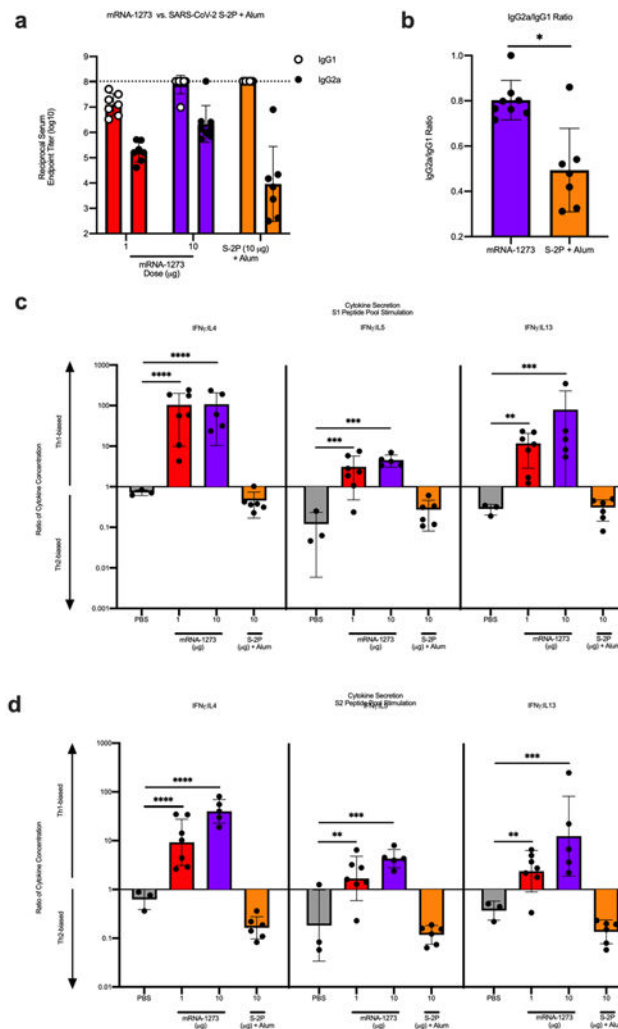


Extended Data Figure 6. A single dose of mRNA-1273 elicits robust antibody responses. BALB/cJ mice (n=10/group) were immunized with 0.01 (green), 0.1 (blue), 1 µg (red), or 10 µg (purple) of mRNA-1273. Sera were collected 2 (unfilled circles) and 4 (filled circles) weeks post-immunization and assessed for SARS-CoV-2 S-specific total IgG by ELISA (a) and neutralizing antibodies against homotypic SARS-CoV-2 pseudovirus (b). (c) S-specific IgG2a and IgG1 were also measured by ELISA, and IgG2a to IgG1 subclass ratios were calculated. (a-b) Timepoints were compared within each dose level by two-sided Wilcoxon signed-rank test, and doses were compared 4 weeks post-boost by Kruskal-Wallis ANOVA with Dunn’s multiple comparisons test. * = p-value < 0.05, ** = p-value < 0.01, *** = p-value < 0.001, **** = p-value < 0.0001. (c) Doses were compared by two-sided Mann-Whitney test, and no significance was found. Data are presented as GMT +/- geometric SD (a-b) or mean +/- SD (c), and dotted lines represent assay limits of detection.



Extended Data Figure 7. mRNA-1273 and SAS-adjuvanted S-2P protein elicit both IgG2a and IgG1 subclass S-binding antibodies.

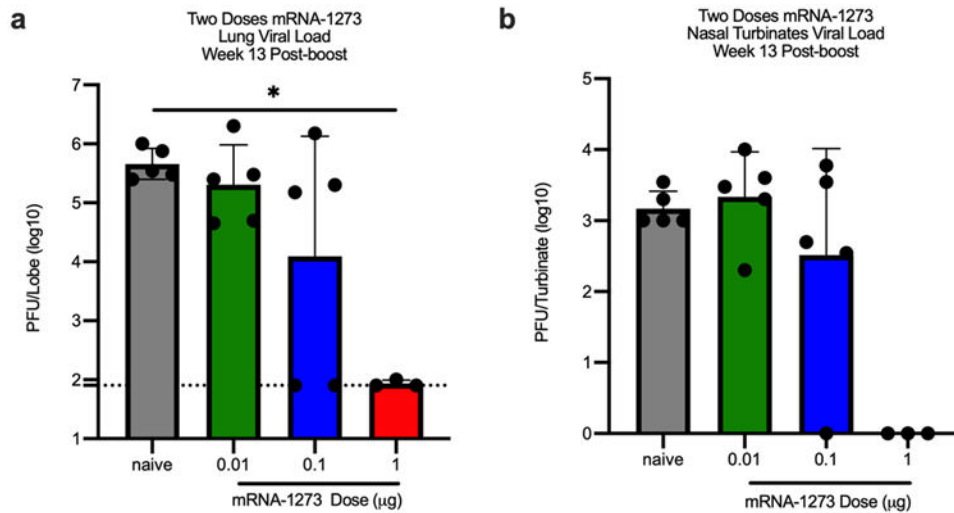
BALB/cJ (a-c) or C57BL/6J (d-f) mice (n=10/group) were immunized at weeks 0 and 3 with 0.01 (green), 0.1 (blue), or 1 μ g (red) of mRNA-1273 or SARS-CoV-2 S-2P protein adjuvanted with SAS. Sera were collected 2 weeks post-boost and assessed by ELISA for SARS-CoV-2 S-specific IgG1 and IgG2a or IgG2c for BALB/cJ and C57BL/6J mice, respectively. Endpoint titers (a-b, d-e) and endpoint titer ratios of IgG2a to IgG1 (c) and IgG2c to IgG1 (f) were calculated. For mice for which endpoint titers did not reach the lower limit of detection (dotted line), ratios were not calculated (N/A). Data are presented as GMT \pm geometric SD (a-b, d-e) or mean \pm SD (c,f).



Extended Data Figure 8. mRNA-1273 elicits Th1-skewed responses compared to S-2P protein adjuvanted with alum.

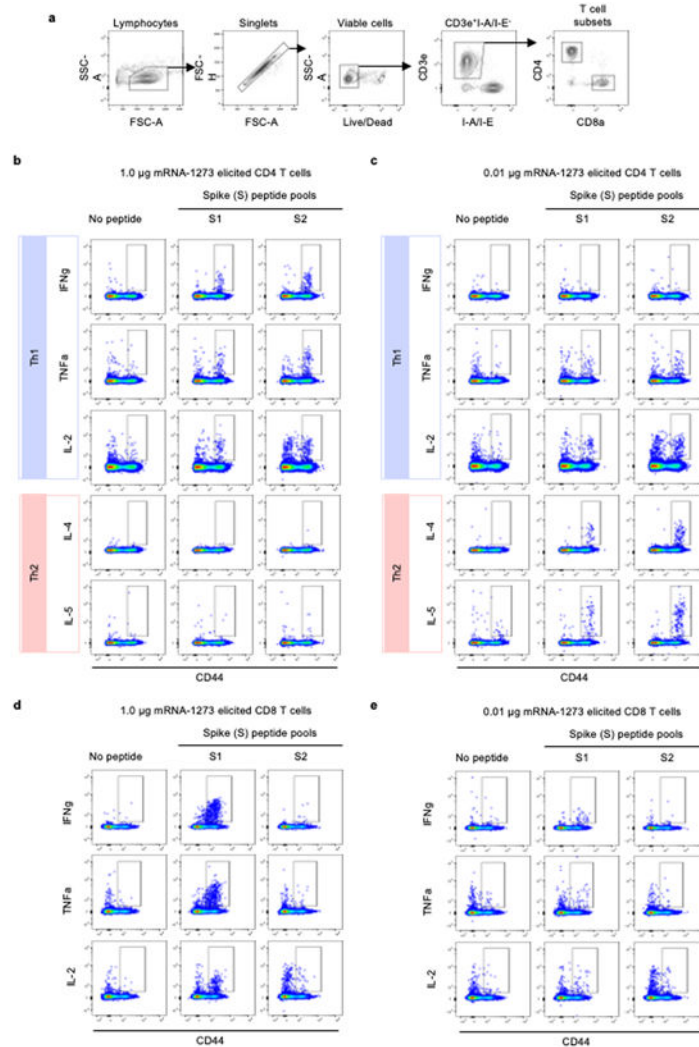
BALB/c mice (n=6/group) were immunized at weeks 0 and 2 weeks with 1 (red) or 10 μ g (purple) of mRNA-1273 or 10 μ g of SARS-CoV-2 S-2P protein adjuvanted with alum hydrogel (orange). Control mice were administered PBS (gray) (n=3). (a-b) Sera were collected 2 weeks post-boost and assessed by ELISA for SARS-CoV-2 S-specific IgG1 and IgG2a. Endpoint titers (a) and endpoint titer ratios of IgG2a to IgG1 (b) were calculated. (c-d) Splenocytes were collected 4 weeks post-boost to evaluate IFN- γ , IL-4, IL-5, and IL-13

cytokine levels secreted by T cells re-stimulated with S1 (c) and S2 (d) peptide pools, measured by Luminex. (b) Immunogens were compared by two-sided Mann-Whitney test. (c-d) For cytokines, all comparisons were compared to PBS control mice by Kruskal-Wallis ANOVA with Dunn's multiple comparisons test. * = p-value < 0.05, ** = p-value < 0.01, *** = p-value < 0.001, **** = p-value < 0.0001. Data are presented as GMT +/- geometric SD (a) or mean +/- SD (b-d). Dotted line represents assay limit of detection.



Extended Data Figure 9. mRNA-1273 protects mice from upper and lower airway SARS-CoV-2 infection, 13 weeks post-boost.

BALB/cJ mice were immunized at weeks 0 and 3 with 0.01 (green), 0.1 (blue), or 1 µg (red) of mRNA-1273. Age-matched naive mice (gray) served as controls. Thirteen weeks post-boost, mice were challenged with mouse-adapted SARS-CoV-2. Two days post-challenge, at peak viral load, mouse lungs (a) and nasal turbinates (b) were harvested from 5 mice per group (3 mice for the 1 µg group) for analysis of viral titers. All dose levels were compared by Kruskal-Wallis ANOVA with Dunn's multiple comparisons test. * = p-value < 0.05. Data are presented as GMT +/- geometric SD. Dotted line represents assay limit of detection.



Extended Data Figure 10. Flow cytometry panel to quantify SARS-CoV-2 S-specific T cells in mice.

(a) Related to Figure 3d-g, hierarchical gating strategy was used to unambiguously identify single, viable CD4⁺ and CD8⁺ T cells. Gating summary of SARS-CoV-2 S-specific (b-c) CD4⁺ and (d-e) CD8⁺ T cells elicited by 0.1 and 1 µg mRNA-1273 immunization. Antigen-specific T cell responses following peptide pool re-stimulation were defined as CD44^{hi}/cytokine⁺. Concatenated files shown were generated using the same number of randomly selected events from each animal across the different stimulation conditions using FlowJo software, v10.6.2.

Supplementary Material

Refer to Web version on PubMed Central for supplementary material.

Authors

Kizzmekia S. Corbett^{1,#}, Darin K. Edwards^{2,#}, Sarah R. Leist^{3,#}, Olubukola M. Abiona¹, Seyhan Boyoglu-Barnum¹, Rebecca A. Gillespie¹, Sunny Himansu², Alexandra Schäfer³, Cynthia T. Ziwawo¹, Anthony T. DiPiazza¹, Kenneth H. Dinnon³, Sayda M. Elbashir², Christine A. Shaw², Angela Woods², Ethan J. Fritch⁴, David R. Martinez³, Kevin W. Bock⁵, Mahnaz Minai⁵, Bianca M. Nagata⁵, Geoffrey B. Hutchinson¹, Kai Wu², Carole Henry², Kapil Bahi², Dario Garcia-Dominguez², LingZhi Ma², Isabella Renzi², Wing-Pui Kong¹, Stephen D. Schmidt¹, Lingshu Wang¹, Yi Zhang¹, Emily Phung^{1,6}, Lauren A. Chang¹, Rebecca J. Loomis¹, Nedim Emil Altaras², Elisabeth Narayanan², Mihir Metkar², Vlad Presnyak², Cuiping Liu¹, Mark K. Louder¹, Wei Shi¹, Kwanyee Leung¹, Eun Sung Yang¹, Ande West³, Kendra L. Gully³, Laura J. Stevens⁷, Nianshuang Wang⁸, Daniel Wrapp⁸, Nicole A. Doria-Rose¹, Guillaume Stewart-Jones², Hamilton Bennett², Gabriela S. Alvarado¹, Martha C. Nason⁹, Tracy J. Ruckwardt¹, Jason S. McLellan⁸, Mark R. Denison⁷, James D. Chappell⁷, Ian N. Moore⁵, Kaitlyn M. Morabito¹, John R. Mascola¹, Ralph S. Baric^{3,4}, Andrea Carfi^{2,*}, Barney S. Graham^{1,*}

Affiliations

¹Vaccine Research Center; National Institute of Allergy and Infectious Diseases; National Institutes of Health; Bethesda, Maryland, 20892; United States of America

²Moderna Inc., Cambridge, MA, 02139; United States of America

³Department of Epidemiology; University of North Carolina at Chapel Hill; Chapel Hill, North Carolina, 27599; United States of America

⁴Department of Microbiology and Immunology, School of Medicine, University of North Carolina at Chapel Hill; Chapel Hill, North Carolina, 27599; United States of America

⁵National Institute of Allergy and Infectious Diseases; National Institutes of Health; Bethesda, Maryland, 20892; United States of America

⁶Institute for Biomedical Sciences, George Washington University, Washington, DC 20052, United States of America

⁷Department of Pediatrics, Vanderbilt University Medical Center, Nashville, Tennessee, 37212; United States of America

⁸Department of Molecular Biosciences; University of Texas at Austin; Austin, Texas, 78712; United States of America

⁹Biostatistics Research Branch, Division of Clinical Research, National Institute of Allergy and Infectious Diseases, National Institutes of Health; Bethesda, Maryland, 20892; United States of America

Acknowledgements

We thank Karin Bok, Kevin Carlton, Masaru Kanekiyo, Robert Seder, and additional members of all included laboratories for critical discussions, advice, and review of the manuscript. We thank Judy Stein and Monique Young

for technology transfer and administrative support, respectively. We thank members of the NIH NIAID VRC Translational Research Program for technical assistance with mouse experiments. We thank Brenda Hartman for assistance with graphics. This work was supported by the Intramural Research Program of the VRC and the Division of Intramural Research, NIAID, NIH (B.S.G), NIH NIAID grant R01-AI127521 (J.S.M.), and NIH grants AI149644 and AI100625 (R.S.B.). We thank Huihui Mu and Michael Farzan for the ACE2-overexpressing 293 cells and Michael Whitt for kind support on VSV-based pseudovirus production. mRNA-1273 has been funded in part with Federal funds from the Department of Health and Human Services, Office of the Assistant Secretary for Preparedness and Response, Biomedical Advanced Research and Development Authority, under Contract 75A50120C00034. PRNT assays were funded under NIH Contract HHSN26120080001E Agreement 17x198 (to J.D.C.), furnished through Leidos Biomedical Research, Inc. MERS-CoV mRNA mouse challenge studies were funded under NIH Contract HHSN2722017000361 Task Order No. 75N93019F00132 Requisition No. 5494549 (to R.B.). K.S.C.'s research fellowship was partially funded by the Undergraduate Scholarship Program, Office of Intramural Training and Education, Office of the Director, NIH. D.R.M. was funded by NIH NIAID grant T32-AI007151 and a Burroughs Wellcome Fund Postdoctoral Enrichment Program Award.

References

1. Pallesen J et al. Immunogenicity and structures of a rationally designed prefusion MERS-CoV spike antigen. *Proceedings of the National Academy of Sciences* 114, E7348–E7357, doi:10.1073/pnas.1707304114 (2017).
2. Korber B et al. Tracking changes in SARS-CoV-2 Spike: evidence that D614G increases infectivity of the COVID-19 virus. *Cell*, doi:10.1016/j.cell.2020.06.043 (2020).
3. Dong E, Du H & Gardner L An interactive web-based dashboard to track COVID-19 in real time. *The Lancet Infectious Diseases* 20, 533–534, doi:10.1016/S1473-3099(20)30120-1 (2020). [PubMed: 32087114]
4. Keni R, Alexander A, Nayak PG, Mudgal J & Nandakumar K COVID-19: Emergence, Spread, Possible Treatments, and Global Burden. *Frontiers in Public Health* 8, doi:10.3389/fpubh.2020.00216 (2020).
5. Graham BS Rapid COVID-19 vaccine development. *Science* 368, 945–946, doi:10.1126/science.abb8923 (2020). [PubMed: 32385100]
6. Graham BS, Gilman MSA & McLellan JS Structure-Based Vaccine Antigen Design. *Annu Rev Med* 70, 91–104, doi:10.1146/annurev-med-121217-094234 (2019). [PubMed: 30691364]
7. McLellan JS et al. Structure of RSV fusion glycoprotein trimer bound to a prefusion-specific neutralizing antibody. *Science* 340, 1113–1117, doi:10.1126/science.1234914 (2013). [PubMed: 23618766]
8. McLellan JS et al. Structure-based design of a fusion glycoprotein vaccine for respiratory syncytial virus. *Science* 342, 592–598, doi:10.1126/science.1243283 (2013). [PubMed: 24179220]
9. Crank MC et al. A proof of concept for structure-based vaccine design targeting RSV in humans. *Science* 365, 505–509 (2019). [PubMed: 31371616]
10. Gilman MSA et al. Rapid profiling of RSV antibody repertoires from the memory B cells of naturally infected adult donors. *Sci Immunol* 1, doi:10.1126/sciimmunol.aaj1879 (2016).
11. Walls AC et al. Cryo-electron microscopy structure of a coronavirus spike glycoprotein trimer. *Nature* 531, 114–117, doi:10.1038/nature16988 (2016). [PubMed: 26855426]
12. Kirchdoerfer RN et al. Pre-fusion structure of a human coronavirus spike protein. *Nature* 531, 118–121, doi:10.1038/nature17200 (2016). [PubMed: 26935699]
13. Graham BS & Sullivan NJ Emerging viral diseases from a vaccinology perspective: preparing for the next pandemic. *Nat Immunol* 19, 20–28, doi:10.1038/s41590-017-0007-9 (2018). [PubMed: 29199281]
14. Graham BS & Corbett KS Prototype pathogen approach for pandemic preparedness: world on fire. *J Clin Invest*, doi:10.1172/JCI139601 (2020).
15. Menachery VD et al. A SARS-like cluster of circulating bat coronaviruses shows potential for human emergence. *Nat Med* 21, 1508–1513, doi:10.1038/nm.3985 (2015). [PubMed: 26552008]
16. Menachery VD et al. SARS-like WIV1-CoV poised for human emergence. *Proc Natl Acad Sci U S A* 113, 3048–3053, doi:10.1073/pnas.1517719113 (2016). [PubMed: 26976607]

17. Graham BS, Mascola JR & Fauci AS Novel Vaccine Technologies: Essential Components of an Adequate Response to Emerging Viral Diseases. *JAMA* 319, 1431–1432, doi:10.1001/jama.2018.0345 (2018). [PubMed: 29566112]
18. Dowd KA et al. Rapid development of a DNA vaccine for Zika virus. *Science* 354, 237–240 (2016). [PubMed: 27708058]
19. Pardi N, Hogan MJ, Porter FW & Weissman D mRNA vaccines - a new era in vaccinology. *Nat Rev Drug Discov* 17, 261–279, doi:10.1038/nrd.2017.243 (2018). [PubMed: 29326426]
20. Hassett KJ et al. Optimization of Lipid Nanoparticles for Intramuscular Administration of mRNA Vaccines. *Mol Ther Nucleic Acids* 15, 1–11, doi:10.1016/j.omtn.2019.01.013 (2019). [PubMed: 30785039]
21. Mauger DM et al. mRNA structure regulates protein expression through changes in functional half-life. *Proceedings of the National Academy of Sciences* 116, 24075, doi:10.1073/pnas.1908052116 (2019).
22. Cockrell AS et al. A mouse model for MERS coronavirus-induced acute respiratory distress syndrome. *Nat Microbiol* 2, 16226–16226, doi:10.1038/nmicrobiol.2016.226 (2016). [PubMed: 27892925]
23. Wrapp D et al. Cryo-EM structure of the 2019-nCoV spike in the prefusion conformation. *Science* 367, 1260–1263, doi:10.1126/science.abb2507 (2020). [PubMed: 32075877]
24. Freeman B et al. Validation of a SARS-CoV-2 spike protein ELISA for use in contact investigations and sero-surveillance. *bioRxiv* (2020).
25. Klumpp-Thomas C et al. Standardization of enzyme-linked immunosorbent assays for serosurveys of the SARS-CoV-2 pandemic using clinical and at-home blood sampling. *medRxiv*, 2020.2005.2021.20109280, doi:10.1101/2020.05.21.20109280 (2020).
26. Kim HW et al. RESPIRATORY SYNCYTIAL VIRUS DISEASE IN INFANTS DESPITE PRIOR ADMINISTRATION OF ANTIGENIC INACTIVATED VACCINE12. *American Journal of Epidemiology* 89, 422–434, doi:10.1093/oxfordjournals.aje.a120955 (1969). [PubMed: 4305198]
27. Fulginiti VA, Eller JJ, Downie AW & Kempe CH Altered Reactivity to Measles Virus: Atypical Measles in Children Previously Immunized With Inactivated Measles Virus Vaccines. *JAMA* 202, 1075–1080, doi:10.1001/jama.1967.03130250057008 (1967). [PubMed: 6072745]
28. Bolles M et al. A Double-Inactivated Severe Acute Respiratory Syndrome Coronavirus Vaccine Provides Incomplete Protection in Mice and Induces Increased Eosinophilic Proinflammatory Pulmonary Response upon Challenge. *Journal of Virology* 85, 12201, doi:10.1128/JVI.06048-11 (2011). [PubMed: 21937658]
29. Czub M, Weingartl H, Czub S, He R & Cao J Evaluation of modified vaccinia virus Ankara based recombinant SARS vaccine in ferrets. *Vaccine* 23, 2273–2279, doi:10.1016/j.vaccine.2005.01.033 (2005). [PubMed: 15755610]
30. Deming D et al. Vaccine efficacy in senescent mice challenged with recombinant SARS-CoV bearing epidemic and zoonotic spike variants.
31. Hou YJ et al. SARS-CoV-2 Reverse Genetics Reveals a Variable Infection Gradient in the Respiratory Tract. *LID - S0092-8674(20)30675-9 [pii] LID - 10.1016/j.cell.2020.05.042 [doi]*.
32. Dinno KH et al. A mouse-adapted SARS-CoV-2 model for the evaluation of COVID-19 medical countermeasures. *bioRxiv*, 2020.2005.2006.081497, doi:10.1101/2020.05.06.081497 (2020).
33. Jackson LA et al. An mRNA Vaccine against SARS-CoV-2 — Preliminary Report. *New England Journal of Medicine*, doi:10.1056/NEJMoa2022483 (2020).
34. Nelson J et al. Impact of mRNA chemistry and manufacturing process on innate immune activation. *Science Advances* 6 (2020).
35. ter Meulen J et al. Human Monoclonal Antibody Combination against SARS Coronavirus: Synergy and Coverage of Escape Mutants. *PLOS Medicine* 3, e237, doi:10.1371/journal.pmed.0030237 (2006). [PubMed: 16796401]
36. John S et al. Multi-antigenic human cytomegalovirus mRNA vaccines that elicit potent humoral and cell-mediated immunity.
37. Bahl K et al. Preclinical and Clinical Demonstration of Immunogenicity by mRNA Vaccines against H10N8 and H7N9 Influenza Viruses. *Molecular Therapy* 25, 1316–1327, doi:10.1016/j.ymthe.2017.03.035 (2017). [PubMed: 28457665]

38. Vogel AB et al. Self-Amplifying RNA Vaccines Give Equivalent Protection against Influenza to mRNA Vaccines but at Much Lower Doses. *Molecular Therapy* 26, 446–455, doi:10.1016/j.ymthe.2017.11.017 (2018). [PubMed: 29275847]
39. Douglas MG, Kocher JF, Scobey T, Baric RS & Cockrell AS Adaptive evolution influences the infectious dose of MERS-CoV necessary to achieve severe respiratory disease. *Virology* 517, 98–107, doi:10.1016/j.virol.2017.12.006 (2018). [PubMed: 29277291]
40. Scobey T et al. Reverse genetics with a full-length infectious cDNA of the Middle East respiratory syndrome coronavirus. *Proceedings of the National Academy of Sciences* 110, 16157, doi:10.1073/pnas.1311542110 (2013).
41. Wang L et al. Evaluation of candidate vaccine approaches for MERS-CoV. *Nature Communications* 6, 7712, doi:10.1038/ncomms8712 (2015).
42. Bottcher E et al. Proteolytic activation of influenza viruses by serine proteases TMPRSS2 and HAT from human airway epithelium. *J Virol* 80, 9896–9898, doi:10.1128/JVI.01118-06 (2006). [PubMed: 16973594]
43. Whitt MA Generation of VSV pseudotypes using recombinant G-VSV for studies on virus entry, identification of entry inhibitors, and immune responses to vaccines. *Journal of virological methods* 169, 365–374, doi:10.1016/j.jviromet.2010.08.006 (2010). [PubMed: 20709108]

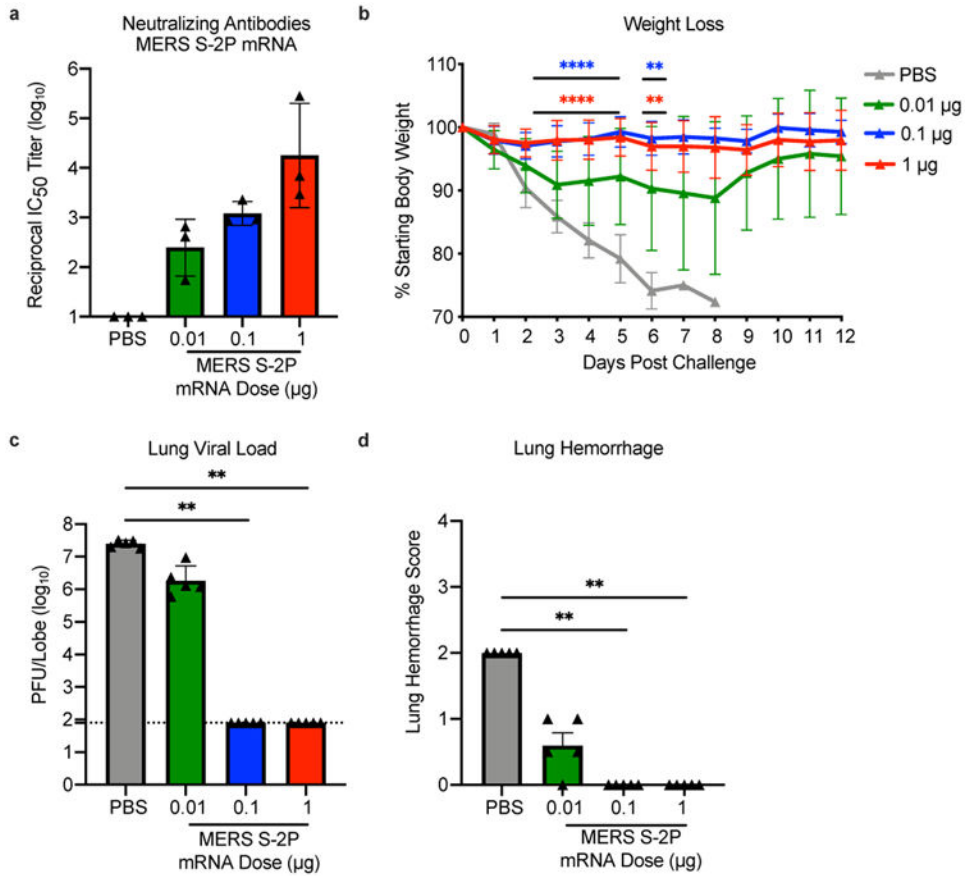


Figure 1. MERS-CoV S-2P mRNA protects mice from lethal challenge. 288/330^{+/+} mice were immunized at weeks 0 and 3 with 0.01 (green), 0.1 (blue), or 1 µg (red) of MERS-CoV S-2P mRNA. Control mice were administered PBS (gray). Two weeks post-boost, sera were collected from 3 mice per group and assessed for neutralizing antibodies against MERS m35c4 pseudovirus (a). Four weeks post-boost, 12 mice per group were challenged with a lethal dose of mouse-adapted MERS-CoV (m35c4). Following challenge, mice were monitored for weight loss (b). Two days post-challenge, at peak viral load, lung viral titers (c) and hemorrhage (0 = no hemorrhage, 4 = severe hemorrhage in all lobes) (d) were assessed from 5 animals per group. (a) Statistical analysis was not performed. (c-d) All dose levels were compared by Kruskal-Wallis ANOVA with Dunn’s multiple comparisons test. (b) For weight loss, all comparisons are to PBS control mice at each timepoint by two-sided Mann-Whitney test. ** = p-value < 0.01, **** = p-value < 0.0001. Data are presented as GMT +/- geometric SD (a,c) or mean +/- SD (b,d). (c) Dotted line represents assay limit of detection.

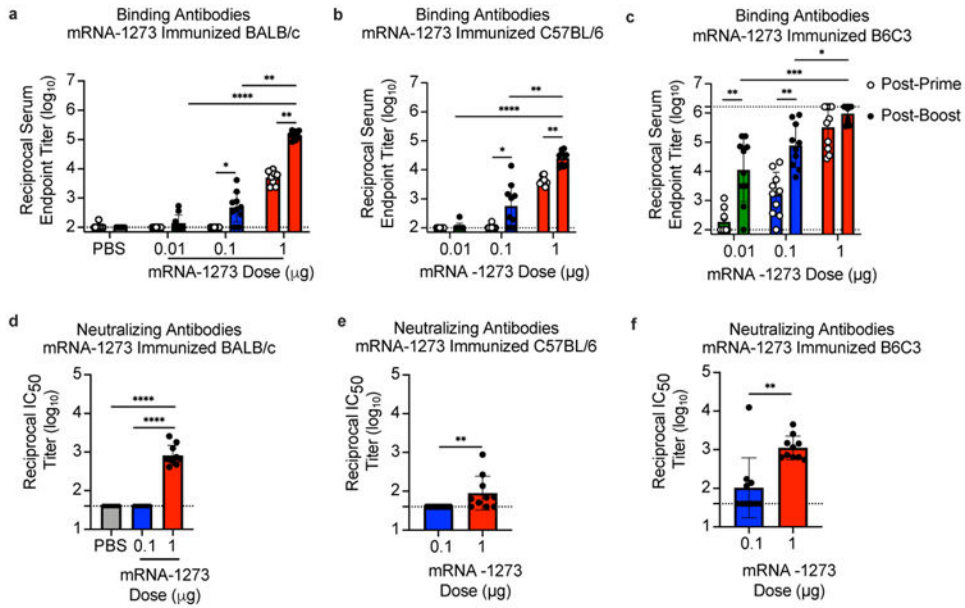


Figure 2. mRNA-1273 elicits robust binding and pseudovirus neutralizing antibody responses in multiple mouse strains.

BALB/cJ (a, d), C57BL/6J (b, e), or B6C3F1/J (c, f) mice (n=10/group) were immunized at weeks 0 and 3 weeks with 0.01 (green), 0.1 (blue), or 1 μg (red) of mRNA-1273. Control BALB/cJ mice were administered PBS (gray). Sera were collected 2 weeks post-prime (unfilled circles) and 2 weeks post-boost (filled circles) and assessed for SARS-CoV-2 S-specific IgG by ELISA (a-c), and, for post-boost sera, neutralizing antibodies against homotypic SARS-CoV-2 pseudovirus (d-f). (a-c) Timepoints were compared within each dose level by two-sided Wilcoxon signed-rank test, and doses were compared post-boost by Kruskal-Wallis ANOVA with Dunn’s multiple comparisons test. (d-f) Vaccine groups were compared by two-sided Mann-Whitney test. * = p-value < 0.05, ** = p-value < 0.01, *** = p-value < 0.001, **** = p-value < 0.0001. Data are presented as GMT +/- geometric SD. Dotted lines represent assay limits of detection.

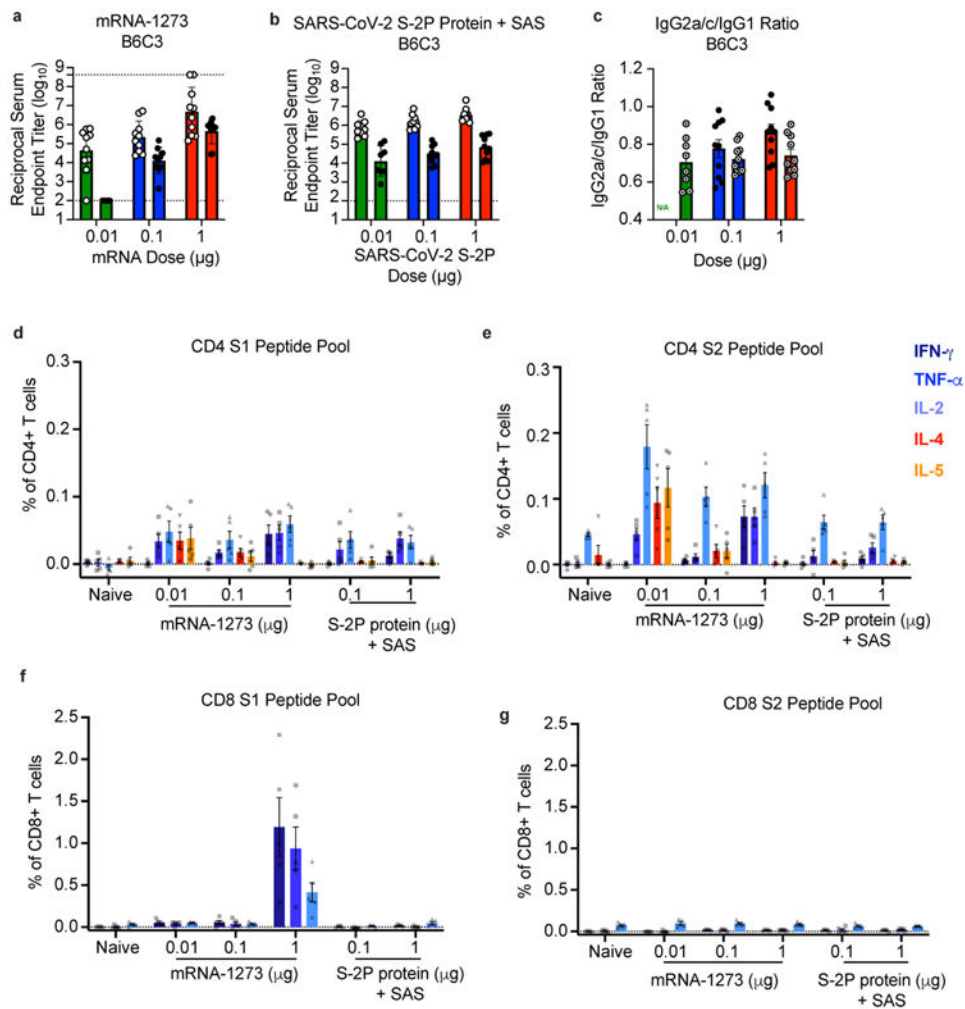


Figure 3. Immunizations with mRNA-1273 and S-2P protein, delivered with TLR4 agonist, elicit S-specific Th1-biased T cell responses.

B6C3F1/J mice ($n=10/\text{group}$) were immunized at weeks 0 and 3 with 0.01, 0.1, or 1 μg of mRNA-1273 or SAS-adjuvanted SARS-CoV-2 S-2P protein. Sera were collected 2 weeks post-boost and assessed by ELISA for SARS-CoV-2 S-specific IgG1 and IgG2a/c. Endpoint titers (a-b) and endpoint titer ratios of IgG2a/c to IgG1 (c) were calculated. For mice for which endpoint titers did not reach the lower limit of detection (dotted line), ratios were not calculated (N/A). (d-g) Seven weeks post-boost, splenocytes were isolated from 5 mice per group and re-stimulated with no peptides or pools of overlapping peptides from SARS-CoV-2 S protein in the presence of a protein transport inhibitor cocktail. After 6 hours, intracellular cytokine staining (ICS) was performed to quantify CD4+ and CD8+ T cell responses. Cytokine expression in the presence of no peptides was considered background and subtracted from the responses measured from the S1 and S2 peptide pools for each individual mouse. (d-e) CD4+ T cells expressing IFN- γ , TNF- α , IL-2, IL-4 and IL-5 in response to the S1 (d) and S2 (e) peptide pools. (f-g) CD8+ T cells expressing IFN- γ , TNF- α , and IL-2 in response to the S1 (f) and S2 (g) peptide pools.

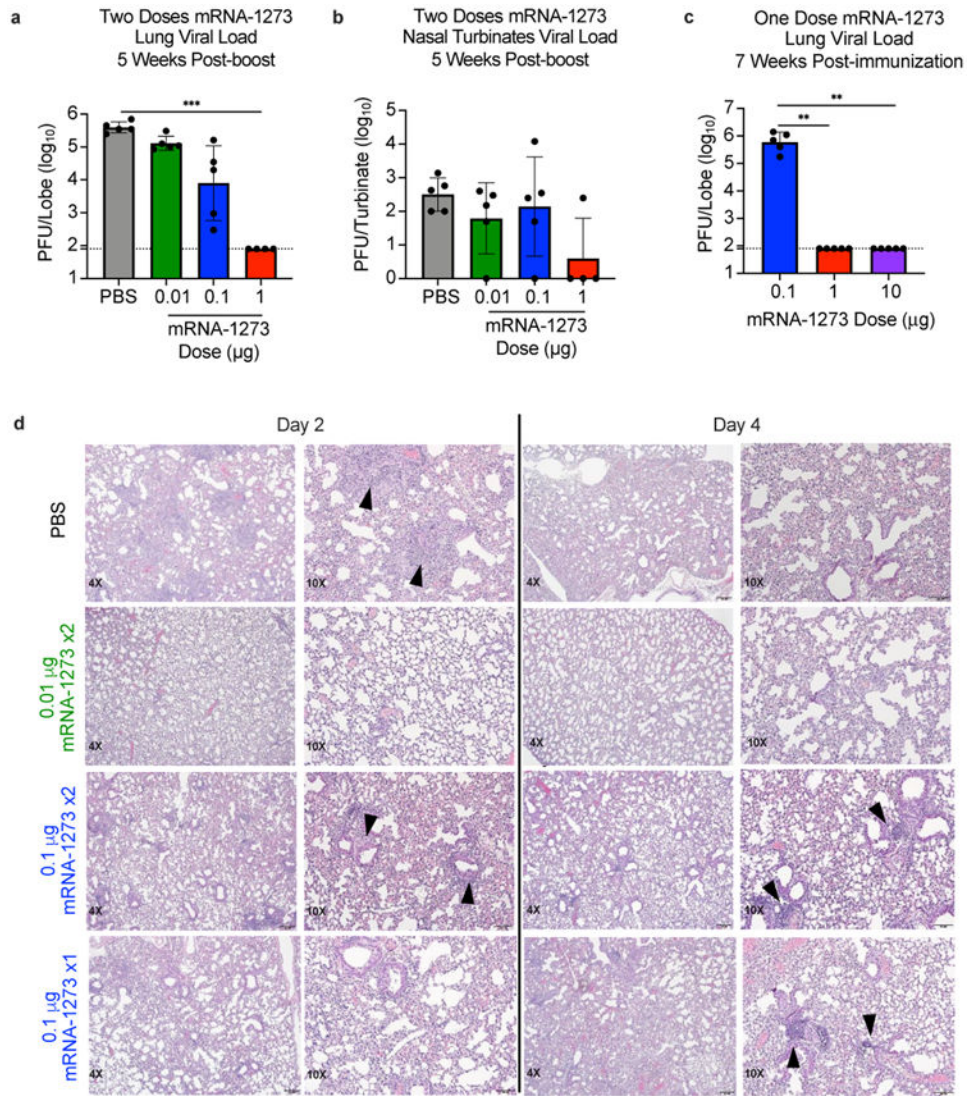


Figure 4. mRNA-1273 protects mice from upper and lower airway SARS-CoV-2 infection. (a-b) BALB/cJ mice ($n=10$ /group) immunized at weeks 0 and 3 with 0.01 (green), 0.1 (blue), or 1 µg (red) of mRNA-1273 or PBS, were challenged with mouse-adapted SARS-CoV-2 five weeks post-boost. (c) Other groups were immunized with single doses of 0.1 (blue), 1 (red), or 10 (purple) µg of mRNA-1273 and challenged 7 weeks post-immunization. Two days post-challenge, at peak viral load, mouse lungs (a,c) and nasal turbinates (b) were harvested from 5 mice/group to measure viral titers. (a-c) Data are presented as GMT+/-geometric SD, and dotted lines represent assay limits-of-detection. Group comparisons were made by Kruskal-Wallis ANOVA with Dunn's multiple comparisons test. **= p -value<0.01, ***= p -value<0.001. (d) At days 2 and 4 post-challenge, Hematoxylin and eosin-stained lung sections were examined from 5 mice per group, and representative photomicrographs (4X and 10X) from each group with detectable virus in lung are shown. Day 2 lungs from PBS control mice demonstrated moderate-to-severe, predominantly neutrophilic, inflammation present within, and surrounding, small bronchioles (arrowheads); alveolar capillaries were markedly expanded by infiltrating inflammatory cells. In the 0.01

μg two-dose group, inflammation was minimal to absent. In the 0.1 μg two-dose group, occasional areas of inflammation intimately associated with small airways (bronchioles) and adjacent vasculature (arrowheads) were seen, primarily composed of neutrophils. In the single-dose 0.1 μg group, there were mild patchy expansion of alveolar septae by mononuclear and polymorphonuclear cells. At day 4, lungs from PBS control mice exhibited moderate to marked expansion of alveolar septae (interstitial pattern) with decreased prominence of adjacent alveolar spaces. In the 0.01 μg two-dose group, inflammation was minimal to absent. Lungs in the 0.1 μg two-dose group showed mild, predominantly lymphocytic inflammation, associated with bronchioles and adjacent vasculature (arrowheads). In the single-dose 0.1 μg group there was mild, predominantly lymphocytic, inflammation around bronchovascular bundles (arrowheads).